IAI Journals.ASM.org

Chlamydia muridarum Induction of Glandular Duct Dilation in Mice

Xin Sun,[a,c] Zhangsheng Yang,[a] Hongbo Zhang,[a,d] Jin Dai,[a] Jianlin Chen,[a,e] Lingli Tang,[a,f] Sheena Rippentrop,[b] Min Xue,[c] Guangming Zhong,[a] Ganqiu Wu[a,g]

Departments of Microbiology and Immunology[a] and Obstetrics and Gynecology,[b] University of Texas Health Science Center at San Antonio, San Antonio, Texas, USA; Department of Obstetrics and Gynecology, 3rd Xiangya Hospital,[c] Departments of Pathology,[d] Obstetrics and Gynecology,[e] and Clinical Diagnosis,[f] 2nd Xiangya Hospital, and Department of Histology and Embryology, Xiangya School of Medicine,[g] Central South University of China, Changsha, Hunan, People's Republic of China

Although *Chlamydia*-induced hydrosalpinx in women and mice has been used as a surrogate marker for tubal infertility, the medical relevance of nontubal pathologies, such as uterine horn dilation, developed in mice following chlamydial infection remains unclear. We now report that the uterine horn dilation correlates with glandular duct dilation detected microscopically following *Chlamydia muridarum* infection. The dilated glandular ducts pushed the uterine horn lumen to closure or dilation and even broke through the myometrium to develop extrusion outside the uterine horn. The severity scores of uterine horn dilation observed macroscopically correlated well with the number of cross sections of the dilated glandular ducts counted under microscopy. Chlamydial infection was detected in the glandular epithelial cells, potentially leading to inflammation and dilation of the glandular ducts. Direct delivery of *C. muridarum* into the mouse uterus increased both uterine horn/glandular duct dilation and hydrosalpinx. However, the chlamydial plasmid, which is essential for the induction of hydrosalpinx, was not required for the induction of uterine horn/glandular duct dilation. Screening 12 strains of mice for uterine horn dilation following *C. muridarum* infection revealed that B10.D2, C57BL/10J, and C57BL/6J mice were most susceptible, followed by BALB/cJ and A/J mice. Deficiency in host genes involved in immune responses failed to significantly alter the *C. muridarum* induction of uterine horn dilation. Nevertheless, the chlamydial induction of uterine horn/glandular duct dilation may be used to evaluate plasmid-independent pathogenicity of *Chlamydia* in susceptible mice.

Chlamydial infection in the lower genital tract can ascend to cause pathologies in the upper genital tract, leading to manifestations such as pelvic inflammatory disease and infertility (1, 2). An extensively investigated pathology is the long-lasting hydrosalpinx that can be induced by *Chlamydia trachomatis* infection in women (3, 4) and *Chlamydia muridarum* infection in female mice (5–9). Thus, the *C. muridarum* mouse genital tract infection model has been extensively used to investigate the mechanisms of *C. trachomatis*-induced hydrosalpinx in women. In addition to hydrosalpinx, dilation of the uterine horn has also been frequently detected in *C. muridarum*-infected mice (6, 7, 10–15). *C. trachomatis* genital tract infection in women is known to induce acute cervical and endometrial pathologies, including cervicitis and endometritis (16–18). However, it is unclear whether the mouse uterine horn dilation model can be used to investigate the pathogenesis of *C. trachomatis*-induced acute endometrial inflammation in women. Thus, it is necessary to characterize the *C. muridarum*-induced uterine horn dilation. Many previous mouse model-based studies grouped both hydrosalpinx and uterine horn dilation as upper genital tract pathology (19, 20) and focused only on the fertility outcome (21–23) or patency of the upper genital tract (6) without differentiating uterine horn dilation from hydrosalpinx (8, 24–28). Although a previous study reported that interferon regulatory transcription factor 3 (IRF3) protected mice from uterine horn pathology during *C. muridarum* infection (13) and efforts have also been made to define host factors involved in *C. muridarum* induction of uterine horn dilation (29), the pathological basis of uterine horn dilation remains unclear. To understand whether and how *C. muridarum* infection induces uterine horn dilation and whether it can be used as a model for investigating *C. trachomatis* pathogenesis, we set out to define the pathological basis of uterine horn dilation in the current study.

Mice have a long duplex uterus, referred to as the uterine horn. The endometrial layer of the uterus/uterine horn consists of a simple columnar lumenal epithelium surrounded by stromal cells containing glands lined by cuboidal glandular epithelium. Mice undergo adenogenesis postnatally by budding from the lumenal epithelium (30). Progesterone has been shown to inhibit uterine gland development in the neonatal mouse uterus (31, 32), while estrogen seems to be required for maintaining uterine gland function in adult mice (33). Aged mice can spontaneously develop cystic endometrial hyperplasia (34), which involves dilation and proliferation of the glandular ducts. The glandular duct cysts vary in size but are restricted within the endometrium. Adenomyosis refers to the invasion of hyperplastic glands into the myometrium (35), which can be difficult to differentiate from endometriosis (36) when the dislocated endometrial tissue is still associated with the uterus. Hydrometra may also cause uterine horn dilation (34), which is, however, due to uterine horn lumenal distension without involving the uterine glands. Finally, uterine tumors with or without gland involvment can cause uterine horn dilation. For example, BALB/c mice commonly develop uterine stromal pol-

Received 11 March 2015 **Returned for modification** 18 March 2015
Accepted 20 March 2015

Accepted manuscript posted online 30 March 2015

Citation Sun X, Yang Z, Zhang H, Dai J, Chen J, Tang L, Rippentrop S, Xue M, Zhong G, Wu G. 2015. *Chlamydia muridarum* induction of glandular duct dilation in mice. Infect Immun 83:2327–2337. doi:10.1128/IAI.00154-15.

Editor: R. P. Morrison

Address correspondence to Guangming Zhong, Zhongg@UTHSCSA.edu, or Ganqiu Wu, wuganqiu@163.com.

doi:10.1128/IAI.00154-15

yps, which consist of polypoid protrusions of the stroma covered with normal uterine mucosa. However, tumor tissues can be differentiated microscopically. Since the causes of mouse uterine pathology are complex and some can occur in the absence of infection, it is important to define the pathological basis of uterine horn dilation in mice infected with *C. muridarum*.

In the current study, we found that the long-lasting uterine horn dilation that developed 60 days after *C. muridarum* infection correlated well with glandular duct dilation. The glandular epithelial cells were highly susceptible to *C. muridarum* infection, and directly inoculating *C. muridarum* into the uteruses of mice increased both the incidence and severity of the glandular duct dilation. However, the chlamydial plasmid, known to be essential for the induction of hydrosalpinx, was not required for the induction of glandular duct dilation. Thus, the dilation of the uterine horn and glandular duct can be a unique pathology distinct from hydrosalpinx, which may be used as a distinct model for evaluating chlamydial pathogenicity.

MATERIALS AND METHODS

***C. muridarum* and mouse infection.** *C. muridarum* organisms were propagated and purified in HeLa229 cells (human cervical carcinoma epithelial cells; ATCC catalog number CCL2) as described previously (37). The wild-type *C. muridarum* strain Nigg was acquired from Robert Brunham at the University of Manitoba (38). The plasmid-free *C. muridarum* strain CMUT3.G5 was derived from the wild-type *C. muridarum* and plaque purified as described previously (15, 39). For *C. muridarum* infection in mice, the organisms were used to infect 6- to 7-week-old female mice via either the intrauterine or intravaginal route with 2×10^5 inclusion-forming units (IFU), as described previously (8, 25, 40). The following strains of wild-type and knockout (KO) mice used in the current study were all purchased from Jackson Laboratories (Bar Harbor, ME): C57BL/6J (JAX [Jackson Laboratories] stock number 000664), BALB/cJ (000651), C3H/HeJ (000659), TRIF KOs (005037), TIRAP KOs (017629), JNK2 KOs (004321), interleukin 1 receptor type I (IL-1R1) KOs (003245), IL-10 KOs (002251), and gamma interferon (IFN-γ) KOs (002287; 2 died before sacrifice). The pathology data for the remaining strains of mice used in the current study were acquired from the images and/or tissues of mice sacrificed in previous studies (8, 15, 24, 26, 28, 41). The infection procedures were as follows. Five days prior to infection, each mouse was injected with 2.5 mg medroxyprogesterone (Depo-Provera; Pharmacia Upjohn, Kalamazoo, MI) subcutaneously to increase mouse susceptibility to infection. Control uninfected mice were also injected with progesterone. After infection, the mice were monitored for vaginal live-organism shedding and sacrificed 60 to 80 days postinfection for observation of gross genital tract pathologies. Some mice were sacrificed on day 7 or 14 postinfection for detection of chlamydial infection in the uterine tissues. The animal experiments were carried out in accordance with the recommendations in the Guide for the Care and Use of Laboratory Animals of the National Institutes of Health. The protocol was approved by the Committee on the Ethics of Laboratory Animal Experiments of the University of Texas Health Science Center at San Antonio.

For monitoring live-organism shedding from swab samples, vaginal/cervical swabs were taken every 3 or 4 days for the first week and then weekly thereafter until negative shedding was observed at 2 consecutive time points. To quantitate live chlamydial organisms, each swab was soaked in 0.5 ml of sucrose-phosphate-glutamic acid (SPG) and vortexed with glass beads, and the chlamydial organisms released into the supernatant were titrated on HeLa cell monolayers in duplicate. The infected cultures were processed for immunofluorescence assay as described below. Inclusions were counted in five random fields per coverslip under a fluorescence microscope. For coverslips with less than 1 IFU per field, entire coverslips were counted. Coverslips showing obvious cytotoxicity of HeLa cells were excluded. The total number of IFU per swab was calculated based on the mean number of IFU per view, number of views per coverslip, dilution factor, magnification, and inoculation volumes. Where possible, a mean number of IFU per swab was derived from the serially diluted and duplicate samples for any given swab. The calculated total number of IFU per swab was converted into $\log_{10}$ units and used to calculate the mean and standard deviation across mice of the same group at each time point.

Mouse genital tract gross pathology evaluation. Mice were sacrificed 60 to 80 days after infection to evaluate both the gross pathology of uterine horn dilation and the histological pathology of glandular duct dilation. Before removing the genital tract tissues from the mice, an *in situ* gross examination was performed under a stereoscope (Olympus, Center Valley, PA) for evidence of hydrosalpinx, uterine horn dilation, and other gross abnormalities. The genital tract tissues were then excised in their entirety from the vagina to the ovary and laid on a blue photography mat for acquisition of digital images. The oviduct hydrosalpinges were visually scored based on their dilation size using a scoring system as described previously (14). For the current study, the genital tract images were used for scoring uterine horn dilation based on the following criteria. Each horn was divided into 4 equal sections or portions. Based on the number of sections occupied by the dilated areas, the horn was scored from 0 to 4: 0, no dilation; 1, horn with visible dilation, but the area was ≤1 section; 2, horn with a dilated area of >1 but ≤2 sections; 3, horn with a dilated area of >2 but ≤3 sections; 4, horn with a dilated area of >3 sections. The sum of the severity scores from both horns of the same mouse were used as the score for the given mouse for subsequent statistical analyses. Mice with any level of identifiable uterine horn dilation were counted as uterine horn dilation positive.

Mouse genital tract histological pathology evaluation. For histological scoring of glandular duct dilation, the excised mouse genital tract tissues were fixed in 10% neutral formalin, embedded in paraffin, and serially sectioned longitudinally at 5-μm widths. Efforts were made to include the cervix, both uterine horns, oviducts, and lumenal structures of each tissue in each section. The sections were stained with hematoxylin and eosin (H&E) as described previously (6). For the current study, the H&E-stained sections were scored for severity of glandular duct dilation by counting the cross sections of dilated glandular ducts in each uterine horn under a 4× objective lens. The counting is straightforward, using the following steps: (i) identify the remaining myometrium in both sides of the uterine horn wall; (ii) try to find the remaining uterine horn lumen with epithelial folds; (iii) try to examine only the uterine and uterine horn regions and avoid the oviduct regions, which should be easy to differentiate. With a clear orientation of the uterine horn structure, the dilated glandular ducts that were large and pushed the rest of the stromal cells toward either the horn lumen or the myometrium or both were conveniently counted as dilated glandular ducts. We did not count the dilated uterine horn lumen, although the horn lumen dilation could be a consequence of the severe glandular duct dilation. We focused only on the dilated glandular ducts to avoid skewing the counting. The dilated horn lumenal epithelium and dilated glandular duct epithelium can be differentiated under a 40× or larger objective lens. Efforts were also made to differentiate the dilated glandular ducts from cystic endometrial hyperplasia, which occurred spontaneously in all mice at the age when the mice were sacrificed in the current study. Although the cystic ducts were larger than the normal glandular ducts, they were much smaller than the dilated ducts associated with chlamydial infection. Most importantly, the cystic ducts were numerous and restricted within the endometrium without significant physical impacts on either the uterine horn lumen epithelium or myometrium. Although some pathologists might diagnose the dilated glandular ducts that were surrounded by smooth muscle cells as adenomyosis, we counted them as dilated glandular ducts because, although adenomyosis can be affected by hormones (35), the mice used in the current study were always sacrificed 60 days or more after injection and the mice were pretreated with progesterone only 5 days prior to infection. In addition, control uninfected mice were also injected with progesterone.

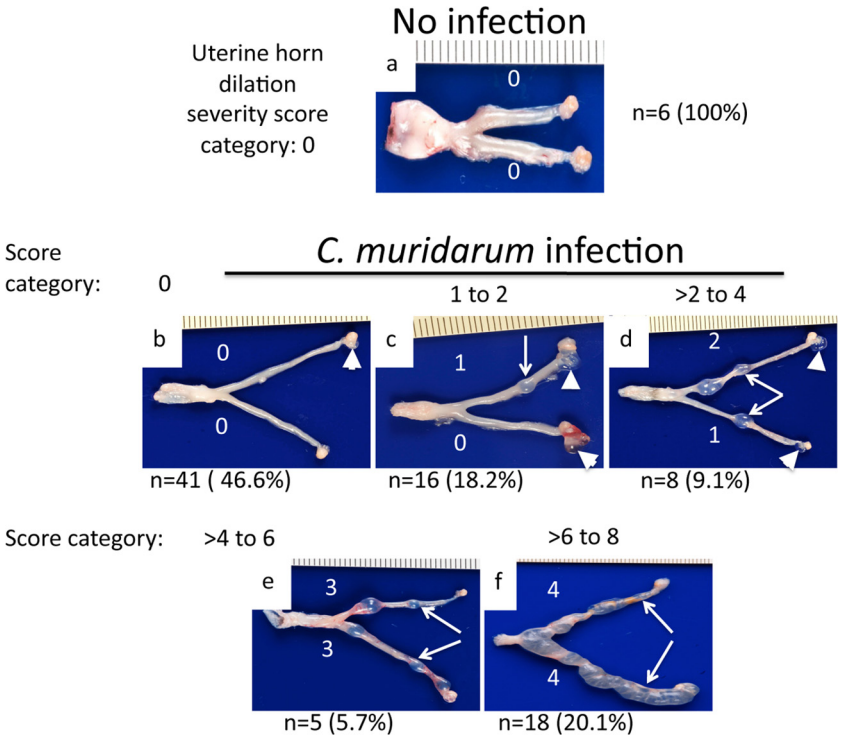

FIG 1 *C. muridarum* induction of uterine horn dilation evaluated macroscopically. (a) C57BL/6J mice were sacrificed on days 60 to 80 after intravaginal inoculation with or without *C. muridarum* for examining upper genital tract pathology, including uterine horn dilation. Based on the portion of the uterine horn occupied by the dilated areas (representative dilation areas in each horn are indicated by arrows) as described in Materials and Methods, the severity of uterine horn dilation was semiquantitatively scored for each uterine horn, as indicated by the white numbers. (b to f) Among the 88 C57BL/6J mice infected with *C. muridarum*, 41 (46.6%) failed to develop any uterine dilation (b) and 16 (18.2%) developed uterine dilation with a severity score of 1 to 2 (c), 8 (9.1%) with a score of >2 to 4 (d), 5 (5.7%) with a score of >4 to 6 (e), and 18 (20.1%) with a score of >6 to 8 (f), as indicated. The hydrosalpinx detected for each oviduct is marked with a white arrowhead. Note that 70 of the 88 mice were from previous studies, and the uterine horn dilation was scored based on stored images from previous studies, as indicated in Table 1. The remaining 18 infected mice and the 6 no-infection controls were from the current study.

More importantly, it is possible that chlamydial infection of the glandular epithelial cells may cause adenomyosis. Since most dilated glandular ducts did not have the typical characteristics of adenomyosis, we decided to use "glandular duct dilation" to describe all dilated glandular ducts potentially induced by chlamydial infection, which may include adenomyosis. The numbers of cross sections counted from both sides of the uterine horns from the same mouse were added to represent the severity of the glandular duct dilation for the given mouse.

Immunofluorescence assay. The sections made from some mouse genital tract tissue blocks as described above were processed for immunohistochemical detection of *C. muridarum* as described previously (12). A primary antibody raised by immunization of rabbits with purified *C. muridarum* elementary bodies (unpublished data) was used to detect *C. muridarum* organisms, which were further visualized with goat anti-rabbit IgG conjugated with Cy2 (green; Jackson ImmunoResearch, West Grove, PA). Hoechst DNA dye (blue; Sigma-Aldrich, St. Louis, MO) was used to visualize nuclei. To localize the chlamydial inclusions in the context of tissue structure, after the immunolabeled sections were subjected to fluorescence microscopy observation and image acquisition, the same sections were further treated with H&E staining (H&E staining removed all fluorescence signals, which was why we took the fluorescence images prior to the H&E staining) to reveal the tissue structure and cellular distribution. In this way, the chlamydial-inclusion-positive cells could be identified in the H&E images. The immunofluorescence images were acquired using an Olympus AX-70 fluorescence microscope equipped with multiple filter sets and Simple PCI imaging software (Olympus) as described previously (37), while the H&E images were acquired under visible light. The images were processed using the Adobe Photoshop program (Adobe Systems, San Jose, CA).

Statistical analyses. The semiquantitative pathology scores were analyzed using the Wilcoxon rank-sum test and the incidence rates using Fisher's exact test. The correlation coefficient was calculated using CORREL in Excel, and its significance was analyzed using the *P* Value Calculator for Correlation Coefficients software from the Free Statistics Calculators website.

RESULTS

***C. muridarum* induces uterine horn dilation in mice following intravaginal infection.** Intravaginal infection with *C. muridarum* is known to induce both uterine horn dilation and oviduct hydrosalpinx. In the current study, we carefully evaluated uterine horn dilation in C57BL/6J mice with or without *C. muridarum* infection (Fig. 1). A scoring scheme consisting of 0 to 4 points per horn (with a maximum of 8 points per mouse) was used to semiquantitatively describe the severity of the uterine horn dilation. We found that none of the 6 C57BL/6J mice without *C. muridarum* infection (but with progesterone pretreatment) developed any significant uterine horn dilation. All 88 C57BL/6J mice intravaginally infected with *C. muridarum* displayed similar levels of live-organism shedding over the time course (data not shown). Forty-seven of the 88 infected mice developed varying degrees of uterine horn dilation: 16 (18.2%) developed uterine dilation with a severity score of up to 2, 8 (9.1%) with a score of >2 to 4, 5 (5.7%) with >4 to 6, and 18 (20.1%) with >6 to 8. Most mice displayed dilation scores in the range of either up to 2 or >6, suggesting that this semiquantitative method can sensitively differentiate varying de-

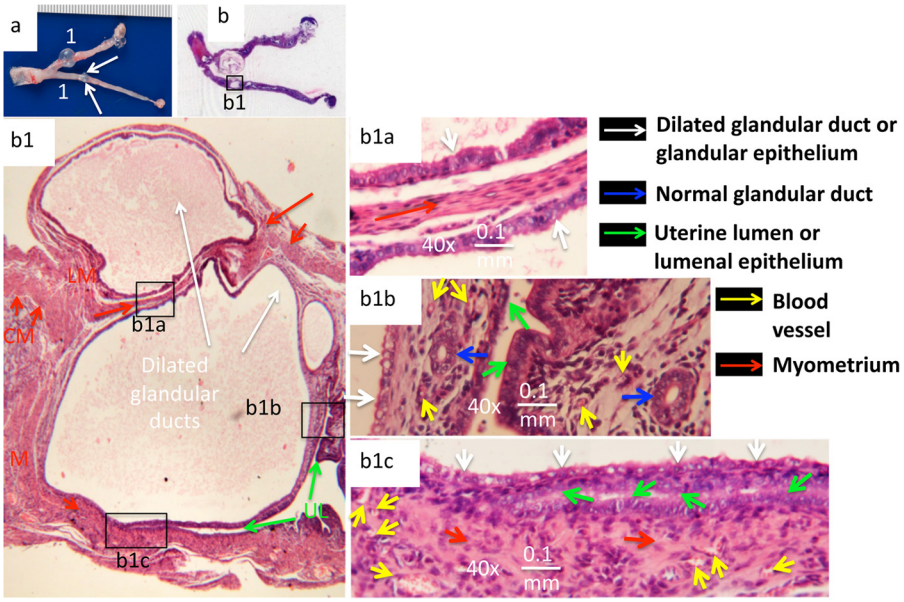

FIG 2 *C. muridarum* induction of glandular duct dilation observed microscopically. (a) Representative genital tract tissue from a mouse with a uterine horn dilation severity score of 2. (b) The corresponding H&E-stained slide was scanned. One of the areas with visually detectable uterine horn dilation (box b1) was subjected to microscopic observation under a 4× objective lens. In the enlargement of the b1 boxed area, the myometrium is labeled with a red M, and the inner circular smooth muscle cells (CM; short red arrows) and the outer longitudinal smooth muscle cells (LM; long red arrows) are differentiated. The uterine horn lumen (UL; green arrows) is labeled. The cross sections of dilated glandular ducts are indicated by white arrows. The three boxed areas were subjected to further microscopic observation under a 40× objective lens. In the enlargement of the b1a boxed area, the white arrows point to the glandular epithelia from two dilated glandular ducts facing in opposite directions. Sandwiched between the two glandular epithelia is a narrow layer of longitudinal smooth muscle (long red arrow). The two glandular epithelia look very similar (white arrows). In the enlargement of the b1b boxed area, the glandular epithelia (the white arrows indicate dilated glandular duct epithelia, and the blue arrows indicate normal glandular ducts) and uterine lumenal epithelia (green arrows) are shown. Normal glandular ducts (blue arrows) and blood vessels (yellow arrows) in the endometria are indicated on both sides of the lumen. However, the dilated glandular duct epithelium (white arrows; mainly consisting of cuboidal epithelial cells) on the left side appeared to be distinctly different from the uterine horn lumenal epithelia (green arrows; ciliated simple columnar epithelial cells can be identified). In the enlargement of the b1c boxed area, another example of two uterine horn epithelia (green arrows) being pushed close to each other by the dilated glandular duct on top (white arrows) is shown. The myometrium (red arrows) is filled with blood vessels (yellow arrows), but no endometrium was identified beneath the bottom lumenal epithelium.

grees of uterine horn dilation. Since >50% of the mice were induced to develop uterine horn dilation by *C. muridarum* infection and none of the uninfected mice developed any significant uterine dilation, we concluded that the uterine horn dilation was induced by *C. muridarum* infection. The hydrosalpinx from the same set of mice was also noted, and some of the results were previously published (8, 15, 26, 28, 41). Although mice with more severe uterine horn dilation seemed to lack hydrosalpinx in the oviduct in some cases, there was no significant correlation between uterine horn dilation and oviduct hydrosalpinx when all 88 mice were taken into consideration. Thus, uterine horn dilation and hydrosalpinx seemed to be two distinct gross pathologies in the upper genital tract induced by lower genital tract infection with *C. muridarum*.

***C. muridarum*-induced uterine horn dilation correlates well with dilated glandular ducts.** Having semiquantitatively evaluated the *C. muridarum*-induced uterine horn dilation, we then carefully examined the dilated uterine horn tissues under microscopy (Fig. 2). The overall structure of the uterine horn with visible dilation could still be clearly identified microscopically under a 4× objective lens, with the myometrium localized between the serosa or perimetrium and the endometrium, or the basement membrane when the endometrium no longer existed. The remaining uterine horn lumen and lumenal epithelium, along with mucosal folds, were also easily localized, although the lumen was no longer contiguous. In the particular tissue shown, two cross sections of dilated glandular ducts were identified, with the larger one below the smaller one. The bottom (larger) one appeared to push the uterine horn lumen below to close, while the top (smaller) dilated duct was already localized outside the muscle layer and extruded beyond the boundary of the uterine horn wall. In addition, the two dilated duct sections appeared to squeeze the muscle layer into a thin strip between them. Further observation under higher magnification (a 40× objective lens) revealed a clear difference in the epithelial structure between the dilated ducts and the uterine horn lumen. The ciliated simple epithelial cells were abundantly associated with the luminal epithelium, while more cuboidal epithelial cells were identified in the glandular epithelium. These observations indicated that the dilated ducts came from the glandular ducts, which was consistent with a common finding that multiple dilated-duct cross sections were detected in the tissue sections cut longitudinally.

To test whether all uterine horn dilation induced by *C. muridarum* infection is a result of glandular duct dilation, we microscopically examined most mouse genital tract tissues used in the current study under a 4× objective lens. The dilated glandular duct cross sections were readily identified as the cause of the uterine horn dilation. As shown in Fig. 3, either a single dilated glandular duct invaded the uterine horn lumen or multiple dilated glandular ducts expanded against both the lumen and myometrium sides. The dilated glandular duct was also found to break

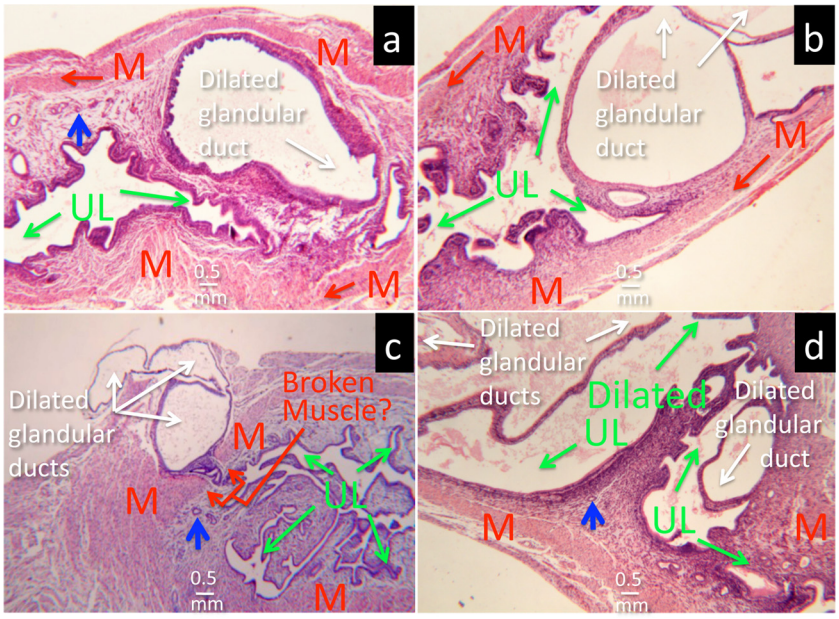

FIG 3 Microscopic identification of cross sections of dilated glandular ducts in dilated uterine horn tissue. (a) A dilated glandular duct pushed the uterine horn lumenal epithelia close together (UL and green arrows). A normal glandular duct (blue arrow) is shown in contrast to the dilated glandular duct. The myometrium (M and red arrows) is marked to orient the overall structure of the uterine horn. (b) Multiple cross sections of dilated glandular ducts. (c) The dilated glandular duct appears to pierce the myometrium and burst outside the uterine horn. (d) The dilated glandular ducts cause dilation of the uterine horn lumen.

through the myometrium and burst outside the uterine horn. In more severe cases, the dilated glandular ducts could both cause the uterine horn lumen to dilate and form protrusions outside the horn. We further semiquantitatively scored the severity of glandular duct dilation by counting the cross sections of dilated glandular ducts in each uterine horn under a 4× objective lens. We found that mice with more severe uterine horn dilation also developed higher glandular duct dilation scores (Fig. 4). The uterine horn dilation was significantly correlated with the number of cross sections of dilated glandular duct detected under microscopy, with a correlation coefficient of 0.87 ($P < 0.01$), which further supported our conclusion that glandular duct dilation forms the structural basis of uterine horn dilation.

***C. muridarum* readily infects glandular duct epithelial cells.** Since we demonstrated above that glandular duct dilation correlates well with uterine horn dilation, we next tested whether the *C. muridarum* organisms could infect glandular duct epithelial cells following intravaginal inoculation. The inoculated C57BL/6 mice were sacrificed on day 7 or 14 for immunohistochemical detection of *C. muridarum* in the genital tract tissues (Fig. 5). Comparison of the H&E staining with immunolabeling of *C. muridarum* organisms allowed us to localize the chlamydial antigen-positive cells. The *C. muridarum* organisms were detected in both the uterine horn lumenal and glandular duct epithelial cells. Further examination of the glandular ducts positive for *C. muridarum* labeling under a 40× objective lens confirmed that the *C. muridarum* inclusions were mainly localized in the glandular epithelial cells. It is worth noting that, although the amount of infection in the luminal epithelial cells was more extensive than that in glandular epithelial cells on day 7 after intravaginal infection, most lumenal epithelial infection was cleared by day 14, which correlated with the presence of massive inflammatory infiltrates in the lumen. Interestingly, the *C. muridarum* infection in the glandular epithelial cells remained intensive on day 14 after infection. The glandular epithelial cells seemed to also produce larger chlamydial inclusions on day 14. These observations implied that the glandular epithelial cells might be more permissive to *C. muridarum* infection.

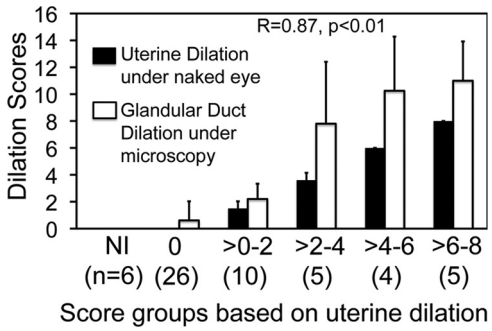

FIG 4 Correlation of uterine horn dilation observed macroscopically with the number of cross sections of dilated glandular duct detected microscopically. The genital tract tissues from 56 of the 94 mice with or without *C. muridarum* infection, as described in the legend to Fig. 1, were examined under a microscope to enumerate the cross sections of dilated glandular tracts. The total number of dilated glandular duct cross sections from both uterine horns of the same mouse was used to semiquantitatively score the severity of glandular duct dilation of that mouse. The glandular duct dilation scores, along with the corresponding uterine horn dilation scores observed with the naked eye, were plotted along the *y* axis. The 56 mice were grouped based on the severity scores of uterine horn dilation as described in the legend to Fig. 1. The mouse groups and the numbers of mice in each group (in parentheses) are shown along the *x* axis. Note that the 6 noninfected (NI) mice failed to develop any uterine horn dilation or glandular duct dilation, and among the 50 infected mice, more severe uterine dilation was always accompanied by more severe glandular duct dilation. The correlation coefficient was 0.87 (CORREL in Excel), with a *P* value of <0.01 (Free Statistics Calculators). The error bars indicate standard deviations.

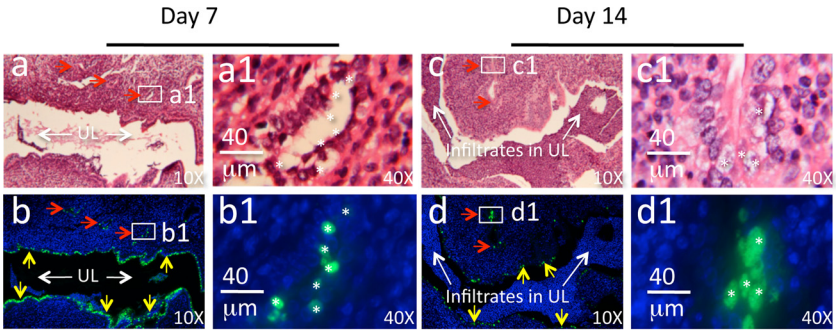

FIG 5 Immunohistochemical detection of *C. muridarum* in glandular duct epithelial cells. C57BL/6 mice intravaginally infected with *C. muridarum* were sacrificed on days 7 (a, a1, b, and b1) and 14 (c, c1, d, and d1) after infection for immunohistochemical detection of *C. muridarum* in the genital tract tissues. The H&E staining images (a and c), taken under a 10× objective lens, revealed the overall structure of the uterine horn with the horn lumen with (c) or without (a) extensive inflammatory infiltration (UL and white arrows) and glandular ducts (a to d, red arrows). The same section was immunofluorescence labeled with an antibody against *C. muridarum* organisms (green) and the Hoechst DNA dye (b, b1, d, and d1, blue) prior to the H&E staining. *C. muridarum* organisms were detected along both the uterine horn lumenal epithelial cells (green inclusions indicated by yellow arrows) and glandular duct epithelial cells (green inclusions indicated by red arrows). A representative glandular duct positive for *C. muridarum* labeling (a to d, white boxes) was selected for further observation under a 40× objective lens (a1 to d1). The locations of some inclusions, marked with white asterisks, from the immunofluorescence-labeled slides (b1 and d1) are indicated in the corresponding H&E slides (a1 and c1), which revealed that the asterisk-marked green inclusions were in the glandular duct epithelial cells.

***C. muridarum* induction of uterine horn/glandular duct dilation is independent of plasmid but can be enhanced by directly inoculating *C. muridarum* organisms into the uterus.** Since the chlamydial cryptic plasmid is a known virulence factor required for *C. muridarum* to induce hydrosalpinx in mice (15, 24, 42), we tested whether the plasmid was also necessary for the induction of uterine horn/glandular duct dilation. When C57BL/6J mice infected with wild-type *C. muridarum* or the plasmid-free *C. muridarum* clone CMUT3.G5 either intravaginally or intrauterinally were observed for upper genital tract pathology, we found that all groups developed significant uterine horn dilation regardless of the organisms used for infection (Fig. 6). The above observation demonstrated that the plasmid-encoded or -regulated virulence factors were not necessary for *C. muridarum* induction of uterine horn/glandular duct dilation. This conclusion is consistent with the observation that the plasmid-free *C. muridarum* organisms also readily infected the glandular duct epithelial cells (Fig. 7), indicating that the plasmid-free organisms possess the same ability to invade glandular duct epithelial cells and potentially cause glandular duct dilation.

Despite the induction of robust uterine horn/glandular duct dilation, the plasmid-free organisms failed to induce any significant hydrosalpinx (Fig. 6), suggesting that uterine dilation and hydrosalpinx are two independent macroscopic pathologies with different degrees of dependence on the plasmid. However, intrauterine infection (by delivering the organisms directly into the upper genital tract) did increase both uterine horn/glandular duct dilation and hydrosalpinx, suggesting that both the uterine and oviduct pathologies are affected by chlamydial ascending infection. These observations together further supported the concept that uterine horn dilation is a unique upper genital tract pathology induced by chlamydial infection and can be used as a pathology marker for studying the plasmid-independent pathogenic mechanisms.

Determining the host factors required for *C. muridarum* induction of uterine horn dilation. We first compared 12 strains of inbred mice for their susceptibilities to *C. muridarum* induction of uterine horn dilation (Table 1). Since uterine horn dilation correlated well with glandular duct dilation, we used only uterine horn

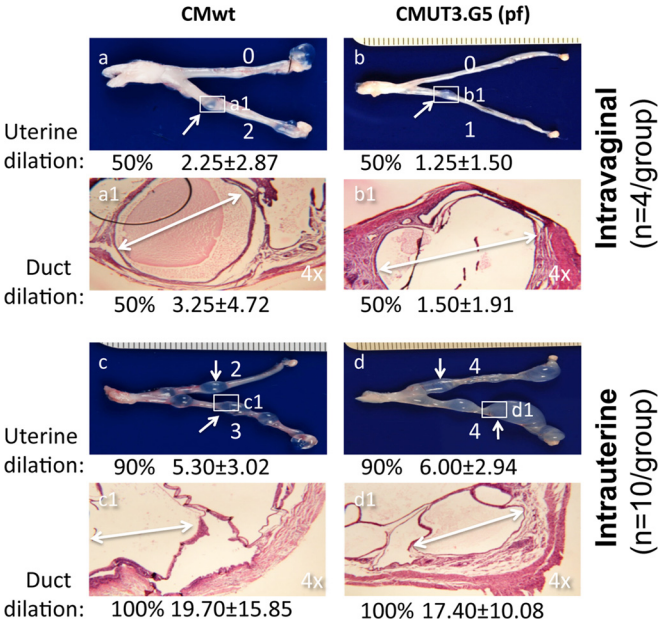

FIG 6 Effect of plasmid depletion and infection routes on *C. muridarum* induction of glandular duct dilation. Four groups of C57BL/6J mice, with 4 mice in each of the first two groups (a, a1, b, and b1) and 10 mice each in the third and fourth groups (c, c1, d, and d1), were infected with wild-type *C. muridarum* (CMwt) (a, a1, c, and c1) or the plasmid-free *C. muridarum* clone CMUT3.G5 (pf) (b, b1, d, and d1) either intravaginally (a, a1, b, and b1) or intrauterinally (c, c1, d, and d1). Sixty days after infection, mice were sacrificed to observe upper genital tract pathology, as described in Materials and Methods. For uterine horn dilation under the naked eye, the white arrows indicate a representative dilated area from each horn, and the dilation severity score for each uterine horn is shown by a white number. To examine glandular duct dilation, the uterine horn dilation lesion areas (boxed and labeled a1 to d1) were subjected to microscopic observation under a 4× objective lens. One representative dilated glandular duct is marked with a white double-headed arrow in each representative H&E image. Both the incidence rates and severity scores of either uterine horn or glandular duct dilation from each group are shown under the corresponding images. Note that 50% or more of the mice developed significant uterine horn and glandular duct dilation regardless of the plasmid deficiency (compare panels a and a1 with b and b1 or c and c1 with d and d1). Intrauterine infection did increase both the incidence rates and severity scores of the dilation (compare panels a and a1 with c and c1 or b and b1 with d and d1).

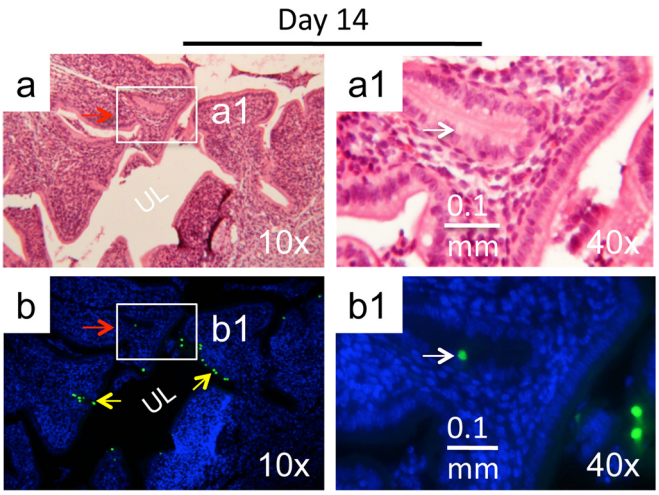

FIG 7 Immunohistochemical detection of plasmid-free *C. muridarum* in glandular duct epithelial cells. C57BL/6 mice intravaginally infected with the plasmid-free *C. muridarum* were sacrificed on day 14 after infection for immunohistochemical detection of *C. muridarum* in the genital tract tissues. (a) The H&E staining images taken under a 10× objective lens revealed the overall structure of the uterine horn, with the horn lumen (UL) marked. (b) The same section was immunofluorescence labeled with an antibody against *C. muridarum* organisms (green) and the Hoechst DNA dye (blue) prior to H&E staining. *C. muridarum* organisms were detected along both the uterine horn lumenal epithelial cells (yellow arrows) and glandular duct epithelial cells (green inclusions indicated by red arrows). (a1 and b1) A representative glandular duct positive for *C. muridarum* labeling (boxes in panels a and b) was selected for further observation under a 40× objective lens. The location of the inclusion marked with a white arrow in the immunofluorescence-labeled slide (b1) is indicated in the H&E slide (a1).

dilation to monitor chlamydial pathogenicity in the upper genital tract in this set of experiments. We found that, following intravaginal infection, the B10.D2, C57BL/10J, and C57BL/6J mice developed the most severe uterine horn dilation, with incidences of 67%, 60%, and 53%, respectively, and mean severity scores of 2.53 or higher; they were followed by BALB/cJ (33%) and A/J (10%) mice. The CBA/J mice developed a minimal level of uterine horn dilation. No uterine horn dilation was induced in the remaining 6 strains (DBA1/J, DBA2/J, SJL/J, C3H/HeN, C3H/HeJ, and NOD/ShiLtJ). The hydrosalinx data from the same mice are also listed in Table 1. It is worth noting that all 12 strains of mice developed hydrosalpinx following *C. muridarum* infection, with CBA/J and SJL/J mice most susceptible while the A/J, DBA/1J, and DBA/2J mice were least susceptible, as described previously (8). There was no significant correlation between the uterine horn dilation and hydrosalpinx.

To further determine the roles of host factors in *C. muridarum* induction of uterine horn dilation, we screened 10 different groups of mice, each with deficiency in one gene involved in either the innate inflammatory or adaptive immune response (Table 2). We found that all the mice, regardless of gene deficiency, developed significant uterine horn dilation following intravaginal infection with *C. muridarum*. The MyD88 KOs and IL-1R1 KOs were most susceptible, followed by the IL-10 KOs, TIRAP KOs, and C5 KOs. However, there was no significant difference between any of these groups and their corresponding controls, suggesting that either additional host factors play more important roles or redundant pathways are involved in *C. muridarum* induction of uterine horn dilation. The hydrosalpinx incidence and severity scores for the mice listed in Table 2 are summarized in Table 3. As reported previously, mice deficient in complement factor C5 failed to develop hydrosalpinx (26), and deficiency in IL-1R1 also significantly reduced the development of hydrosalpinx (43). However, mice deficient in MyD88 developed more severe hydrosalpinx (12). There was no significant alteration in hydrosalpinx development in other gene-deficient mice after *C. muridarum* infection. Again, there was no significant correlation between uterine horn dilation (Table 2) and hydrosalpinx (Table 3).

DISCUSSION

In the current study, we have characterized the pathological basis of the gross pathology of uterine horn dilation by establishing a correlation of glandular duct epithelial cell infection with *C. muridarum* and glandular duct dilation with uterine horn dilation. First, mice similarly pretreated with progesterone without chlamydial infection failed to develop either uterine horn or glandular duct dilation, excluding the possibility of spontaneous uterine horn/glandular duct dilation in the mice used in the current study. Second, glandular duct dilation was always detected in the lesion area, with visible uterine horn dilation from mice intravaginally

TABLE 1 *C. muridarum* induction of uterine horn dilation in 12 strains of mice

Strain	JAX stock no.	No. of mice	Uterine dilation		Hydrosalpinx		Reference or source
			Incidence (%)	Severity	Incidence (%)	Severity	
B10.D2-Hc1 H2d H2-T18c/nSnJ	000463	24	66.7	4.04 ± 3.38	41.7	1.33 ± 1.79	26
C57BL/10J	000665	5	60	3.40 ± 3.51	60.0	2.40 ± 3.29	8
C57BL/6J	000664	88	53.4	2.53 ± 3.11	67.9	3.52 ± 2.81	8 ($n = 3$), 41 ($n = 19$), 15 ($n = 15$), 28 ($n = 25$), 26 ($n = 8$), current study ($n = 18$)
BALB/cJ	000651	86	32.6	1.62 ± 2.77	75.6	3.14 ± 2.85	15 ($n = 7$), current study ($n = 79$)
A/J	000646	10	10	0.60 ± 1.90	10.0	0.40 ± 1.26	8
CBA/J	000656	20	0.05	0.10 ± 0.45	90.0	4.95 ± 2.67	15 ($n = 10$), 8 ($n = 10$)
C3H/HeJ	000659	32	0	0	80.6	3.56 ± 2.45	15 ($n = 24$), 24 ($n = 3$), current study ($n = 5$)
DBA/1J	000670	20	0	0	20.0	0.45 ± 0.94	40 ($n = 6$), 8 ($n = 14$)
SJL/J	000686	15	0	0	80.0	5.00 ± 3.12	15 ($n = 10$), 8 ($n = 5$)
DBA/2J	000671	10	0	0	30.0	0.60 ± 1.07	8
NOD/ShiLtJ	001976	5	0	0	40.0	0.80 ± 1.10	8
C3H/HeN	CR HeNCrl	5	0	0	40.0	2.00 ± 3.46	8

TABLE 2 Effect of host gene deficiency on *C. muridarum* induction of uterine horn dilation

Mouse group	JAX stock no.	KO group			Wild-type controls[a]			Reference or source
		Total no. of mice	Uterine horn dilation		Total no. of mice	Uterine horn dilation		
			%	Score		%	Score	
MyD88 KO	009088	10	70	4 ± 3.49	9	66.7	3.67 ± 3.43	12
TIRAP KO	017629	9	77.8	4.67 ± 3.43	11	54.6	2.64 ± 3.53	Current study
TLR2 KO	004650	14	64.3	3.00 ± 3.21				28
TRIF KO	005037	11	36.4	2.00 ± 3.10				Current study
JNK2 KO	004321	15	33.3	1.33 ± 2.19	14	57.1	1.50 ± 2.24	Current study
C3 KO	003641	8	62.5	2.63 ± 3.16	8	50	1.75 ± 2.76	26
C5 KO	000461	23	69.6	4.61 ± 3.58	24	66.7	4.00 ± 3.28	26
IL-1R1 KO	003245	10	80	6.40 ± 3.73	10	80	6.20 ± 3.29	Current study
IL-10 KO	002251	5	80	4.60 ± 2.97	5	60	1.60 ± 1.67	Current study
IFN-γ KO	002287	3	66.7	1.67 ± 2.08				Current study

[a] JAX no. 000664 for all except C5 KO control (000461).

infected with *C. muridarum*, although mild glandular duct dilation might not be sufficient to cause visible uterine horn dilation. The visible uterine horn dilation was correlated with glandular duct dilation. Third, following an intravaginal infection with *C. muridarum*, the severity of uterine horn dilation was significantly correlated with the severity of glandular duct dilation, suggesting that the semiquantitative scores we established for the two are interchangeable. Fourth, induction of both uterine horn and glandular duct dilations was independent of the chlamydial plasmid but was enhanced by intrauterine inoculation, further strengthening the correlation between the two dilations. Finally, the glandular epithelial cells were not only permissive to *C. muridarum* infection, but also allowed the *C. muridarum* organisms to survive longer in the glandular duct. The plasmid-free *C. muridarum* organisms both infected glandular duct epithelial cells and induced glandular duct dilation. The organisms in the glandular epithelial cells might be more difficult to clear than those in the lumenal epithelial cells. These observations and analyses together suggest that it is possible for *C. muridarum* to induce inflammatory blockage in the glandular duct and cause dilation of the glandular duct, finally resulting in visible uterine horn dilation that lasts for a long time (more than 60 days).

Endometrial glands can be affected by hormones (30, 35, 44). In the current study, all mice were pretreated with progesterone 5 days prior to chlamydial infecton. The question is whether the injected progesterone contributed to the *C. muridarum*-induced dilation of the uterine horn/glandular duct. It is unlikely that the long-lasting uterine horn/glandular duct dilation observed in the current study was caused by the pretreatment with progesterone, because the same strain of mice without chlamydial infection but with similar progesterone pretreatment failed to develop any significant uterine horn or glandular duct dilation when examined 65 days after the pretreatment (Fig. 1). In addition, many other strains of mice, including C3H/Hej, C3H/Hen, DBA/1J and -2J, SJL/J, and NOD/ShiltJ, all failed to develop uterine dilation despite both pretreatment with progesterone and infection with *C. muridarum* (Table 1). Thus, induction of uterine horn dilation seems to be determined by both the host genetics and chlamydial infection, but not the progesterone administered 65 days earlier. This conclusion does not conflict with the general assumption that mice both pretreated with progesterone and infected with *C. muridarum* develop more robust upper genital tract pathologies than those only infected with *C. muridarum*. This is because the progesterone pretreatment can significantly promote sexually transmitted infections by suppressing host immune responses (45). Thus, the progesterone may contribute to chlamydial induction of the uterine horn/glandular duct dilation and hydrosalpinx by increasing mouse susceptibility to *C. muridarum* infection in the upper genital tract. This assumption is supported by the observation that live infection in the upper genital tract is required

TABLE 3 Effect of host gene deficiency on *C. muridarum* induction of hydrosalpinx

Mouse group	Jax stock no.	KO group			Wild-type controls[a]			Reference or source
		Total no. of mice	Hydrosalpinx		Total no. of mice	Hydrosalpinx		
			%	Score		%	Score	
MyD88 KO	009088	10	90	4.2 ± 3.08	9	55.6	1.78 ± 2.05	12
TIRAP KO	017629	9	77.8	4.11 ± 3.33	11	67.7	3.4 ± 3.49	Current study
TLR2 KO	004650	14	64.3	2.36 ± 1.98				28
TRIF KO	005037	11	63.6	2.91 ± 3.02				Current study
JNK2 KO	004321	15	73.3	4.40 ± 3.40	14	85.7	4.07 ± 2.43	Current study
C3 KO	003641	8	87.5	4.63 ± 2.83	8	87.5	3.75 ± 2.43	26
C5 KO	000461	23	0.0	0 ± 0	24	41.7	1.33 ± 1.79	
IL-1R1 KO	003245	10	30.0	1.00 ± 1.73	10	50.0	2.60 ± 3.27	Current study
IL-10 KO	002251	5	80.0	1.80 ± 1.10	5	80.0	3.20 ± 1.79	Current study
IFN-γ KO	002287	3	66.7	5.33 ± 4.62				Current study

[a] JAX no. 000664 for all except C5 KO control (000461).

for *C. muridarum* induction of pathologies in the upper genital tract (9, 15). Although there is an association of the use of the progesterone receptor modulators (as contraceptives) with inactive endometrium cyst-dilated glands in women (44), there has been no direct evidence of the induction of uterine horn/glandular duct dilation in mice by progesterone. On the contrary, progesterone has been shown to inhibit uterine gland development in the neonatal mouse uterus (31, 32), while estrogen seems to be required for maintaining uterine gland function in adult mice (33). Since glandular duct dilation was detected 60 days after infection while the control mice pretreated similarly with progesterone but without infection failed to develop any significant glandular duct dilation (Fig. 1), we can conclude that the long-lasting uterine glandular duct dilation observed in the current study is likely caused by chlamydial infection.

Both uterine horn dilation and oviduct hydrosalpinx have been frequently observed in mice infected with *C. muridarum*. Many previous studies have focused only on hydrosalpinx (5–7, 15, 24, 42), due to the fact that hydrosalpinx observed in women under laparoscopy correlates with tubal factor infertility (46). The current study has correlated uterine horn dilation with glandular duct dilation, which has laid the foundation for further addressing whether the *C. muridarum*-induced uterine horn dilation has any relevance to *C. trachomatis* pathogenesis in women. Although no women have ever been diagnosed with glandular duct dilation, diseases that involve glandular duct dilation, such as adenomyosis, are quite common in women (47). Adenomyosis is an important clinical challenge in gynecology. Hysterectomy is often used to treat fully developed adenomyosis in premenopausal and perimenopausal women. The question is whether *C. trachomatis* infection in women has anything to do with adenomyosis. So far, there is no epidemiological evidence for a linkage between *C. trachomatis* infection and adenomyosis because no studies on the subject have ever been carried out. However, absence of evidence does not necessarily represent evidence of absence. Our current mouse data seem to suggest that it may be worth the effort to investigate the possible association of chlamydial infection with uterine adenomyosis. This suggestion is supported by the observation that *C. trachomatis* infection in the genital tract has also been shown to induce endometrial histopathologies in women (16, 17). Neutrophil infiltration was found in the lumen of endometrial glands in women with upper genital tract infection (16).

The next question is how chlamydial infection induces the dilation of the uterine glandular duct. Defining the chlamydial virulence factors and host determinants that contribute to the *C. muridarum* induction of glandular duct dilation will help advance our understanding of chlamydial pathogenicity. Although the plasmid is necessary for *C. muridarum* induction of hydrosalpinx (15, 42) and the plasmid-encoded Pgp3 is a key virulence factor (24), we found that *C. muridarum* induction of glandular duct dilation was independent of the chlamydial plasmid. This finding is significant in the following 3 respects. First, the fact that the chlamydial plasmid is required for the induction of oviduct hydrosalpinx but not glandular duct dilation suggests that the plasmid may play a more important role in promoting *C. muridarum* ascension from the uterus into the oviduct rather than from the lower genital tract into the uterus. This is because both pathologies require adequate numbers of live organisms to reach to the corresponding tissue sites. Second, the plasmid-encoded factors may contribute more significantly to tubal inflammation than the inflammation in the uterine glandular ducts, which suggests that uterine glandular duct dilation and hydrosalpinx may involve different host mechanisms. Third, the uterine/glandular dilation independence of plasmid may allow us to use this model to evaluate the roles of virulence factors encoded in the chlamydial chromosome in chlamydial pathogenesis in the absence of interference from the plasmid-encoded factors. Interestingly, although intravaginal inoculation of human *C. trachomatis* in mice induced only minimal pathologies in the upper genital tract, intrauterine inoculation of *C. trachomatis* induced very extensive uterine horn dilation (48). This observation is consistent with one of our findings, that intrauterine infection can enhance the induction of uterine horn/glandular duct dilation, and also suggests that the uterine horn dilation model may be used to study *C. trachomatis* pathogenesis in mice. More importantly, the ability of *C. trachomatis* infection to induce robust uterine horn dilation in mice may suggest a potential association of *C. trachomatis* infection with uterine pathologies involving glandular duct dilation, such as adenomyosis in women.

To identify the host factors required for *C. muridarum* induction of uterine horn dilation, we compared 12 different strains of inbred mice and found that B10.D2, C57BL/10J, and C57BL/6J mice were most susceptible, followed by BALB/cJ, A/J, and CBA/J mice. However, no significant uterine dilation was induced in the remaining mice, including DBA1/J, DBA2/J, SJL/J, C3H/HeN, C3H/HeJ, and NOD/ShiLtJ mice. This susceptibility profile was different from the susceptibility to hydrosalpinx induction, since both C3H/HeJ and SJL/J mice were among the strains highly susceptible to developing hydrosalpinx upon chlamydial infection (8). These comparisons and analyses have provided additional evidence that uterine horn dilation is a unique disease distinct from hydrosalpinx. When 10 different groups of mice, each with deficiency in one gene involved in either the innate inflammatory or adaptive immune response, were screened for *C. muridarum* induction of uterine horn dilation, all the mice, regardless of gene deficiency, developed significant uterine horn dilation following intravaginal infection with *C. muridarum*, suggesting that either additional host factors play more important roles or redundant pathways are involved in *C. muridarum* induction of uterine horn dilation. Thus, much more effort is still required to define host factors participating in the *C. muridarum* induction of uterine horn dilation in mice. More information on how *C. muridarum* induces uterine horn dilation in mice should facilitate the investigation of the association of glandular dilation or adenomyosis with *C. trachomatis* infection in women.

ACKNOWLEDGMENT

This work was supported in part by grants (to G. Zhong) from the U.S. National Institutes of Health.

REFERENCES

1. **Brunham RC, Maclean IW, Binns B, Peeling RW.** 1985. Chlamydia trachomatis: its role in tubal infertility. J Infect Dis **152:**1275–1282. http://dx.doi.org/10.1093/infdis/152.6.1275.
2. **Budrys NM, Gong S, Rodgers AK, Wang J, Louden C, Shain R, Schenken RS, Zhong G.** 2012. Chlamydia trachomatis antigens recognized in women with tubal factor infertility, normal fertility, and acute infection. Obstet Gynecol **119:**1009–1016. http://dx.doi.org/10.1097/AOG.0b013e3182519326.
3. **Rodgers AK, Budrys NM, Gong S, Wang J, Holden A, Schenken RS, Zhong G.** 2011. Genome-wide identification of Chlamydia trachomatis

antigens associated with tubal factor infertility. Fertil Steril **96:**715–721. http://dx.doi.org/10.1016/j.fertnstert.2011.06.021.
4. **Sharma M, Sethi S, Daftari S, Malhotra S.** 2003. Evidence of chlamydial infection in infertile women with fallopian tube obstruction. Indian J Pathol Microbiol **46:**680–683.
5. **de la Maza LM, Pal S, Khamesipour A, Peterson EM.** 1994. Intravaginal inoculation of mice with the Chlamydia trachomatis mouse pneumonitis biovar results in infertility. Infect Immun **62:**2094–2097.
6. **Shah AA, Schripsema JH, Imtiaz MT, Sigar IM, Kasimos J, Matos PG, Inouye S, Ramsey KH.** 2005. Histopathologic changes related to fibrotic oviduct occlusion after genital tract infection of mice with Chlamydia muridarum. Sex Transm Dis **32:**49–56. http://dx.doi.org/10.1097/01.olq.0000148299.14513.11.
7. **Cotter TW, Ramsey KH, Miranpuri GS, Poulsen CE, Byrne GI.** 1997. Dissemination of Chlamydia trachomatis chronic genital tract infection in gamma interferon gene knockout mice. Infect Immun **65:**2145–2152.
8. **Chen J, Zhang H, Zhou Z, Yang Z, Ding Y, Zhou Z, Zhong E, Arulanandam B, Baseman J, Zhong G.** 2014. Chlamydial induction of hydrosalpinx in 11 strains of mice reveals multiple host mechanisms for preventing upper genital tract pathology. PLoS One **9:**e95076. http://dx.doi.org/10.1371/journal.pone.0095076.
9. **Zhang H, Zhou Z, Chen J, Wu G, Yang Z, Zhou Z, Baseman J, Zhang J, Reddick RL, Zhong G.** 2014. Lack of long lasting hydrosalpinx in A/J mice correlates with rapid but transient chlamydial ascension and neutrophil recruitment in the oviduct following intravaginal inoculation with Chlamydia muridarum. Infect Immun **82:**2688–2696. http://dx.doi.org/10.1128/IAI.00055-14.
10. **Darville T, Andrews CW, Jr, Laffoon KK, Shymasani W, Kishen LR, Rank RG.** 1997. Mouse strain-dependent variation in the course and outcome of chlamydial genital tract infection is associated with differences in host response. Infect Immun **65:**3065–3073.
11. **Pal S, Hui W, Peterson EM, de la Maza LM.** 1998. Factors influencing the induction of infertility in a mouse model of Chlamydia trachomatis ascending genital tract infection. J Med Microbiol **47:**599–605. http://dx.doi.org/10.1099/00222615-47-7-599.
12. **Chen L, Lei L, Chang X, Li Z, Lu C, Zhang X, Wu Y, Yeh IT, Zhong G.** 2010. Mice deficient in MyD88 develop a Th2-dominant response and severe pathology in the upper genital tract following Chlamydia muridarum infection. J Immunol **184:**2602–2610. http://dx.doi.org/10.4049/jimmunol.0901593.
13. **Prantner D, Sikes JD, Hennings L, Savenka AV, Basnakian AG, Nagarajan UM.** 2011. Interferon regulatory transcription factor 3 protects mice from uterine horn pathology during Chlamydia muridarum genital infection. Infect Immun **79:**3922–3933. http://dx.doi.org/10.1128/IAI.00140-11.
14. **Peng B, Lu C, Tang L, Yeh IT, He Z, Wu Y, Zhong G.** 2011. Enhanced upper genital tract pathologies by blocking Tim-3 and PD-L1 signaling pathways in mice intravaginally infected with Chlamydia muridarum. BMC Infect Dis **11:**347. http://dx.doi.org/10.1186/1471-2334-11-347.
15. **Lei L, Chen J, Hou S, Ding Y, Yang Z, Zeng H, Baseman J, Zhong G.** 2014. Reduced live organism recovery and lack of hydrosalpinx in mice infected with plasmid-free Chlamydia muridarum. Infect Immun **82:**983–992. http://dx.doi.org/10.1128/IAI.01543-13.
16. **Kiviat NB, Wolner-Hanssen P, Eschenbach DA, Wasserheit JN, Paavonen JA, Bell TA, Critchlow CW, Stamm WE, Moore DE, Holmes KK.** 1990. Endometrial histopathology in patients with culture-proved upper genital tract infection and laproscopically diagnosed acute salpingitis. Am J Surg Pathol **14:**167–175. http://dx.doi.org/10.1097/00000478-199002000-00008.
17. **Kiviat NB, Paavonen JA, Wølner-Hanssen P, Critchlow CW, Stamm WE, Douglas J, Eschenbach DA, Corey LA, Holmes KK.** 1990. Histopathology of endocervical infection caused by Chlamydia trachomatis, herpes simplex virus, Trichomonas vaginalis, and Neisseria gonorrhoeae. Hum Pathol **21:**831–837. http://dx.doi.org/10.1016/0046-8177(90)90052-7.
18. **Workowski KA, Berman S, CDC.** 2010. Sexually transmitted diseases treatment guidelines, 2010. MMWR Recomm Rep **59:**1–110.
19. **Cheng W, Shivshankar P, Li Z, Chen L, Yeh IT, Zhong G.** 2008. Caspase-1 contributes to Chlamydia trachomatis-induced upper urogenital tract inflammatory pathologies without affecting the course of infection. Infect Immun **76:**515–522. http://dx.doi.org/10.1128/IAI.01064-07.
20. **Chen L, Cheng W, Shivshankar P, Lei L, Zhang X, Wu Y, Yeh IT, Zhong G.** 2009. Distinct roles of CD28- and CD40 ligand-mediated costimulation in the development of protective immunity and pathology during Chlamydia muridarum urogenital infection in mice. Infect Immun **77:**3080–3089. http://dx.doi.org/10.1128/IAI.00611-08.
21. **Khamesipour A, Pal S, Peterson EM, de la Maza LM.** 1994. Induction of infertility by the Chlamydia trachomatis mouse pneumonitis biovar in strains of mice that differ in their response to the 60 kDa heat shock protein. J Reprod Fertil **101:**287–294. http://dx.doi.org/10.1530/jrf.0.1010287.
22. **Pal S, Peterson EM, de la Maza LM.** 1996. Intranasal immunization induces long-term protection in mice against a Chlamydia trachomatis genital challenge. Infect Immun **64:**5341–5348.
23. **Pal S, Peterson EM, de la Maza LM.** 2005. Vaccination with the Chlamydia trachomatis major outer membrane protein can elicit an immune response as protective as that resulting from inoculation with live bacteria. Infect Immun **73:**8153–8160. http://dx.doi.org/10.1128/IAI.73.12.8153-8160.2005.
24. **Liu Y, Huang Y, Yang Z, Sun Y, Gong S, Hou S, Chen C, Li Z, Liu Q, Wu Y, Baseman J, Zhong G.** 2014. Plasmid-encoded Pgp3 is a major virulence factor for Chlamydia muridarum to induce hydrosalpinx in mice. Infect Immun **82:**5327–5335. http://dx.doi.org/10.1128/IAI.02576-14.
25. **Tang L, Zhang H, Lei L, Gong S, Zhou Z, Baseman J, Zhong G.** 2013. Oviduct infection and hydrosalpinx in DBA1/j mice is induced by intracervical but not intravaginal inoculation with Chlamydia muridarum. PLoS One **8:**e71649. http://dx.doi.org/10.1371/journal.pone.0071649.
26. **Yang Z, Conrad T, Zhou Z, Chen J, Dutow P, Klos A, Zhong G.** 2014. Complement factor C5 but not C3 contributes significantly to hydrosalpinx development in mice infected with Chlamydia muridarum. Infect Immun **82:**3154–3163. http://dx.doi.org/10.1128/IAI.01833-14.
27. **Lu C, Zeng H, Li Z, Lei L, Yeh IT, Wu Y, Zhong G.** 2012. Protective immunity against mouse upper genital tract pathology correlates with high IFNgamma but low IL-17 T cell and anti-secretion protein antibody responses induced by replicating chlamydial organisms in the airway. Vaccine **30:**475–485. http://dx.doi.org/10.1016/j.vaccine.2011.10.059.
28. **Dong X, Liu Y, Chang X, Lei L, Zhong G.** 2014. Signaling via tumor necrosis factor receptor 1 but not Toll-like receptor 2 contributes significantly to hydrosalpinx development following Chlamydia muridarum infection. Infect Immun **82:**1833–1839. http://dx.doi.org/10.1128/IAI.01668-13.
29. **Byrne G.** 2014. Mapping host factors involved in *Chlamydia muridarum* induction of upper genital tract pathologies using BXD mice, p 261–264. *In* Proceedings of the Thirteenth International Symposium on Human Chlamydial Infections, Pacific Grove, CA, 22–27 June 2014. International Chlamydia Symposium, San Francisco, CA.
30. **Cooke PS, Spencer TE, Hayashi K.** 2013. Uterine glands: development, function and experimental model systems. Mol Hum Reprod **19:**547–558. http://dx.doi.org/10.1093/molehr/gat031.
31. **Filant J, Zhou H, Spencer TE.** 2012. Progesterone inhibits uterine gland development in the neonatal mouse uterus. Biol Reprod **86:**1–9. http://dx.doi.org/10.1095/biolreprod.111.097089.
32. **Filant J, Spencer TE.** 2013. Endometrial glands are essential for blastocyst implantation and decidualization in the mouse uterus. Biol Reprod **88:**93. http://dx.doi.org/10.1095/biolreprod.113.107631.
33. **Nanjappa MK, Medrano TI, March AG, Cooke PS.** 2015. Neonatal uterine and vaginal cell proliferation and adenogenesis are independent of estrogen receptor 1 (ESR1) in the mouse. Biol Reprod **92:**78. http://dx.doi.org/10.1095/biolreprod.114.125724.
34. **Dixon D, Alison R, Bach U, Colman K, Foley GL, Harleman JH, Haworth R, Herbert R, Heuser A, Long G, Mirsky M, Regan K, Van Esch E, Westwood RF, Vidal J, Yoshida M.** 2014. Nonproliferative and proliferative lesions of the rat and mouse female reproductive system. J Toxicol Pathol **27:**1S–107S. http://dx.doi.org/10.1293/tox.27.1S.
35. **Parrott E, Butterworth M, Green A, White INH, Greaves P.** 2001. Adenomyosis—a result of disordered stromal differentiation. Am J Pathol **159:**623–630. http://dx.doi.org/10.1016/S0002-9440(10)61733-6.
36. **Rogers PAW, D'Hooghe TM, Fazleabas A, Giudice LC, Montgomery GW, Petraglia F, Taylor RN.** 2013. Defining future directions for endometriosis research: workshop report from the 2011 World Congress of Endometriosis in Montpellier, France. Reprod Sci **20:**483–499. http://dx.doi.org/10.1177/1933719113477495.
37. **Fan T, Lu H, Hu H, Shi L, McClarty GA, Nance DM, Greenberg AH, Zhong G.** 1998. Inhibition of apoptosis in chlamydia-infected cells: blockade of mitochondrial cytochrome c release and caspase activation. J Exp Med **187:**487–496. http://dx.doi.org/10.1084/jem.187.4.487.

38. **Read TD, Brunham RC, Shen C, Gill SR, Heidelberg JF, White O, Hickey EK, Peterson J, Utterback T, Berry K, Bass S, Linher K, Weidman J, Khouri H, Craven B, Bowman C, Dodson R, Gwinn M, Nelson W, DeBoy R, Kolonay J, McClarty G, Salzberg SL, Eisen J, Fraser CM.** 2000. Genome sequences of Chlamydia trachomatis MoPn and Chlamydia pneumoniae AR39. Nucleic Acids Res **28:**1397–1406. http://dx.doi.org/10.1093/nar/28.6.1397.
39. **Liu Y, Chen C, Gong S, Hou S, Qi M, Liu Q, Baseman J, Zhong G.** 2014. Transformation of Chlamydia muridarum reveals a role for Pgp5 in suppression of plasmid-dependent gene expression. J Bacteriol **196:**989–998. http://dx.doi.org/10.1128/JB.01161-13.
40. **Tang L, Yang Z, Zhang H, Zhou Z, Arulanandam B, Baseman J, Zhong G.** 2014. Induction of protective immunity against Chlamydia muridarum intracervical infection in DBA/1j mice. Vaccine **32:**1407–1413. http://dx.doi.org/10.1016/j.vaccine.2013.10.018.
41. **Zeng H, Gong S, Hou S, Zou Q, Zhong G.** 2012. Identification of antigen-specific antibody responses associated with upper genital tract pathology in mice infected with Chlamydia muridarum. Infect Immun **80:**1098–1106. http://dx.doi.org/10.1128/IAI.05894-11.
42. **O'Connell CM, Ingalls RR, Andrews CW, Jr, Scurlock AM, Darville T.** 2007. Plasmid-deficient Chlamydia muridarum fail to induce immune pathology and protect against oviduct disease. J Immunol **179:**4027–4034. http://dx.doi.org/10.4049/jimmunol.179.6.4027.
43. **Nagarajan UM, Sikes JD, Yeruva L, Prantner D.** 2012. Significant role of IL-1 signaling, but limited role of inflammasome activation, in oviduct pathology during Chlamydia muridarum genital infection. J Immunol **188:**2866–2875. http://dx.doi.org/10.4049/jimmunol.1103461.
44. **Dinh A, Sriprasert I, Williams AR, Archer DF.** 14 January 2015. A review of the endometrial histologic effects of progestins and progesterone receptor modulators in reproductive age women. Contraception http://dx.doi.org/10.1016/j.contraception.2015.01.008.
45. **Beagley KW, Gockel CM.** 2003. Regulation of innate and adaptive immunity by the female sex hormones oestradiol and progesterone. FEMS Immunol Med Microbiol **38:**13–22. http://dx.doi.org/10.1016/S0928-8244(03)00202-5.
46. **Rodgers AK, Wang J, Zhang Y, Holden A, Berryhill B, Budrys NM, Schenken RS, Zhong G.** 2010. Association of tubal factor infertility with elevated antibodies to Chlamydia trachomatis caseinolytic protease P. Am J Obstet Gynecol **203:**494.e497–494.e414. http://dx.doi.org/10.1016/j.ajog.2010.06.005.
47. **Taran FA, Stewart EA, Brucker S.** 2013. Adenomyosis: epidemiology, risk factors, clinical phenotype and surgical and interventional alternatives to hysterectomy. Geburtshilfe Frauenheilkd **73:**924–931. http://dx.doi.org/10.1055/s-0033-1350840.
48. **Gondek DC, Olive AJ, Stary G, Starnbach MN.** 2012. CD4+ T cells are necessary and sufficient to confer protection against Chlamydia trachomatis infection in the murine upper genital tract. J Immunol **189:**2441–2449. http://dx.doi.org/10.4049/jimmunol.1103032.